

J-Bio NMR 095

## Protein dynamics studied by rotating frame $^{15}\text{N}$ spin relaxation times

T. Szyperski, P. Luginbühl, G. Otting, P. Güntert and K. Wüthrich\*

*Institut für Molekularbiologie und Biophysik, Eidgenössische Technische Hochschule-Hönggerberg,  
CH-8093 Zürich, Switzerland*

Received 2 October 1992

Accepted 3 December 1992

**Keywords:** Protein dynamics; Basic pancreatic trypsin inhibitor; Nuclear magnetic resonance spectroscopy; Rotating frame spin relaxation times

---

### SUMMARY

Conformational rate processes in aqueous solutions of uniformly  $^{15}\text{N}$ -labeled pancreatic trypsin inhibitor (BPTI) at 36 °C were investigated by measuring the rotating frame relaxation times of the backbone  $^{15}\text{N}$  spins as a function of the spin-lock power. Two different intramolecular exchange processes were identified. A first local rate process involved the residues Cys<sup>38</sup> and Arg<sup>39</sup>, had a correlation time of about 1.3 ms, and was related to isomerization of the chirality of the disulfide bond Cys<sup>14</sup>-Cys<sup>38</sup>. A second, faster motional mode was superimposed on the disulfide bond isomerization and was tentatively attributed to local segmental motions in the polypeptide sequence - Cys<sup>14</sup> - Ala<sup>15</sup> - Lys<sup>16</sup> -. The correlation time for the overall rotational tumbling of the protein was found to be 2 ns, using the assumption that relaxation is dominated by dipolar coupling and chemical shift anisotropy modulated by isotropic molecular reorientation.

---

### INTRODUCTION

Nitrogen-15 spin relaxation in peptide groups is mainly due to dipolar interactions with the amide proton and to chemical shift anisotropy interactions (Allerhand et al., 1971), so that relaxation times can be related to the spatial reorientation of the vector connecting the  $^{15}\text{N}$  nucleus and the amide proton. Therefore, studies of  $^{15}\text{N}$  relaxation times are an attractive approach for investigating global and local motional processes in the backbone of polypeptide chains. For example, the  $^{15}\text{N}$  relaxation times of peptide bonds that are rigidly embedded in a

---

\*To whom correspondence should be addressed.

**Abbreviations:** BPTI, basic pancreatic trypsin inhibitor; 2D, two-dimensional; COSY, 2D correlation spectroscopy; TOCSY, 2D total correlation spectroscopy; RF, radio frequency; CW, continuous wave; TPPI, time-proportional phase incrementation; CSA, chemical shift anisotropy;  $T_1$ , longitudinal relaxation time;  $T_2$ , transverse relaxation time;  $T_{1\rho}$ , relaxation time in the rotating frame  $\tau_R$ , correlation time for overall rotational reorientation of the protein;  $\tau_{\text{ex}}^s$ ,  $\tau_{\text{ex}}^f$ , correlation times for two conformational exchange processes (slow and fast).

regular secondary structure, such as a  $\beta$ -sheet or an  $\alpha$ -helix, can be related to the correlation time for overall rotational tumbling of the molecule. Additional motional processes in other regions of the polypeptide chain can then be identified by comparing the observed relaxation times with those in the more rigid core formed by the regular secondary structures. For such studies with  $^{15}\text{N}$ , a technical advantage arises because, even in uniformly  $^{15}\text{N}$ -labeled proteins, measurements of relaxation times are not disturbed by scalar couplings to other heteronuclei. Two-dimensional heteronuclear NMR techniques efficiently measure longitudinal and transverse  $^{15}\text{N}$  relaxation times (Kay et al., 1987, 1992; Sklenar et al., 1987; Nirmala and Wagner, 1988, 1989; Peng and Wagner, 1992). Kay et al. (1989) recently used relaxation times in conjunction with measurements of heteronuclear  $^1\text{H}$ - $^{15}\text{N}$  Overhauser effects to determine the correlation time for overall rotational tumbling and, following the model-free approach of Lipari and Szabo (1982), the order parameter,  $S$ , for a large number of backbone  $^{15}\text{N}$  nuclei in staphylococcal nuclease. A similar approach has been used by Stone et al. (1992) for domain IIA of glucose permease from *Bacillus subtilis*, by Kördel et al. (1992) for calbindin  $\text{D}_{9\text{K}}$ , by Schneider et al. (1992) for human ubiquitin and, introducing a second-order parameter to describe fast intramolecular motions, by Clore et al. (1990) for interleukin-1 $\beta$ .

Conformational exchange can provide an adiabatic relaxation pathway for transverse magnetization (Kaplan and Fraenkel, 1980; Sandström, 1982). Deverell et al. (1970) showed that relaxation times in the rotating frame,  $T_{1\rho}$ , can be used to determine exchange rate constants, since the efficiency of relaxation of transverse magnetization locked along an effective magnetic field depends on the amplitude of the spin-lock field. Early applications of this principle with small molecules included determination of the rate constant for ring inversion in cyclohexane from measurements of  $T_{1\rho}$  of the ring protons as a function of the spin-lock power, and evaluation of the rotational barriers in a series of urea derivatives on the basis of measurements of  $T_{1\rho}$  of the  $^{13}\text{C}$  nuclei (Stilbs and Moseley, 1978). In BPTI, it was previously noted that some of the proton resonances in the polypeptide segments of residues 14–18 and 36–41 are broadened at 36 °C, so that only few NOEs with these protons could be detected (Wagner and Wüthrich, 1982; Wagner et al., 1987; Berndt et al., 1992). Furthermore, measurements of  $^{13}\text{C}$  spin relaxation times provided evidence for exchange between multiple conformations near the reactive site of BPTI (Wagner and Nirmala, 1989). There is a dynamic equilibrium between two conformational states with different chirality of the Cys<sup>14</sup>–Cys<sup>38</sup> disulfide bond (Otting, G., Liepinsh, E. and Wüthrich, K., unpublished results). While separate resonances for the two conformers could be resolved over the temperature range 4 °C to about 20 °C, the lines coalesced at 36 °C. In the present investigation we used nitrogen-15  $T_{1\rho}$  relaxation data of uniformly  $^{15}\text{N}$ -labeled BPTI at 36 °C to determine the correlation time for overall rotational tumbling of BPTI, and to investigate the frequencies of the local motional processes near the residues Cys<sup>14</sup> and Cys<sup>38</sup>.

Analytical expressions for the determination of the overall rotational tumbling correlation time of a molecule,  $\tau_R$ , from  $T_{1\rho}$  relaxation times have been derived for dipolar relaxation (Blicharski, 1972; Jones, 1966; Peng et al., 1991a), quadrupolar relaxation, and spin-rotation relaxation (Blicharski, 1972). We have derived a corresponding expression for chemical shift anisotropy (CSA) relaxation, which is identical to the one recently published by Peng and Wagner (1992). Using this expression, we investigated the relative contribution of dipolar relaxation and of CSA relaxation to the overall relaxation times, which enabled a refined determination of the correlation time for overall rotational tumbling from  $^{15}\text{N}$   $T_{1\rho}$  measurements.

## THEORY

### *Influence of conformational exchange on $T_{1\rho}$*

As discussed by Peng and Wagner (1992), the equation  $T_{1\rho} = T_2$  in the on-resonance limit, where the effective magnetic field in the rotating frame is transverse, is valid only if there is no evolution of antiphase magnetization of the  $^{15}\text{N}$  nuclei with respect to the amide protons, and if there are no rate processes leading to significant variations in the spectral density functions in the kHz frequency range. The contribution of such exchange processes with frequencies near the Larmor frequency of the applied RF spin-lock field,  $\omega_1$ , to the spectral density function can be determined by carrying out a series of measurements with variable spin-lock power. The contribution of chemical exchange processes to  $T_{1\rho}$  was evaluated earlier for a system of spins that exchange between two equally populated sites with chemical shifts  $\Delta\Omega/2$  and  $-\Delta\Omega/2$  relative to the  $^{15}\text{N}$  carrier frequency,  $\omega_0$  (Eq. 5 in Deverell et al., 1970). Following Deverell et al. (1970) and using the general N-site jump model by Oppenheim et al. (1977), an analogous expression for  $1/T_{1\rho}$  is obtained for the more general situation where the exchange process is between two sites, A and B, with arbitrary populations,  $p_A$  and  $p_B$ , and with rate constants,  $k_{A\rightarrow B}$  and  $k_{B\rightarrow A}$  (Brüschweiler, 1992):

$$\frac{1}{T_{1\rho}} = p_A p_B \Delta\Omega^2 \frac{\tau_{\text{ex}}}{1 + (\omega_1 \tau_{\text{ex}})^2} + \frac{1}{T_{1\rho}^\infty} \quad (1)$$

$\Delta\Omega = \Omega_A - \Omega_B$ , where  $\Omega_A$  and  $\Omega_B$  are the chemical shifts of the spins in the sites A and B (in  $\text{rad s}^{-1}$ ), respectively, relative to the  $^{15}\text{N}$  carrier frequency.  $\omega_1$  is related to the applied RF spin-lock field,  $B_1$ , by  $\omega_1 = -\gamma_N B_1$  and  $T_{1\rho}^\infty$  is the relaxation time for an infinitely large spin-lock power. The equation for the detailed balance,  $p_A k_{A\rightarrow B} = p_B k_{B\rightarrow A} = k/2$ , connects the rate constants and the correlation time,  $\tau_{\text{ex}}$ , of the exchange process, yielding

$$\tau_{\text{ex}} = \frac{2p_A p_B}{k} = \frac{1-p_A}{k_{A\rightarrow B}} \quad (2)$$

As Eq. 1 is derived in the framework of time-dependent perturbation theory up to second-order, it is valid only for  $\Delta\Omega\tau_{\text{ex}} \ll 1$  (see p.282 and p.517 of Abragam, 1961; Deverell et al., 1970). Another limitation of Eq. 1 arises because off-resonance effects are neglected. However, if both of these conditions are fulfilled, measurements of  $T_{1\rho}$  as a function of  $\omega_1$  and subsequent fitting of the data according to Eq. 1 yields values for  $\tau_{\text{ex}}$ ,  $1/T_{1\rho}^\infty$ , and the product  $p_A p_B \Delta\Omega^2$ .

Once the rapid-exchange condition,  $\Delta\Omega\tau_{\text{ex}} \ll 1$ , is violated, the use of second-order perturbation theory is a priori no longer warranted, e.g., higher-order terms may have to be considered (see p.282 of Abragam, 1961). We therefore checked the results obtained from perturbation theory and the possible influence of off-resonance effects by solving the equation of motion in the rotating frame, where the radiofrequency field is static along the x-axis, for an ensemble of  $n$  non-interacting spins under the influence of the Hamiltonian in Eq. 3, where  $n$  is a large number and  $\hbar \equiv 1$ ,

$$H(t) = \sum_{j=1}^n H_j(t) \quad \text{with} \quad H_j(t) = \omega_{1j} I_{jx} + \Omega_j(t) I_{jz}. \quad (3)$$

For the spin  $j$ ,  $I_{jx}$  and  $I_{jz}$  denote Cartesian spin operators. In order to account for spatial inhomogeneity,

genities of the spin-lock field, we assumed that the  $\omega_{ij}$  values ( $j = 1, \dots, n$ ) are independent random variables which are uniformly distributed within the interval  $[0.75 \omega_1, 1.25 \omega_1]$ .  $\Omega_j(t)$  describes the Zeeman interaction, which is a function of time because of the exchange between the conformations A and B:

$$\Omega_j(t) = \begin{cases} \Omega_A, & \text{if spin } j \text{ is in conformation A at time } t; \\ \Omega_B, & \text{if spin } j \text{ is in conformation B at time } t; \end{cases} \quad (4)$$

We assumed that the exchange events of different individual spins are not correlated, and that the exchange reactions  $A \rightarrow B$  and  $B \rightarrow A$  occur with the rates  $k_{A \rightarrow B}$  and  $k_{B \rightarrow A}$ , respectively. Therefore, the lifetimes,  $\tau$ , of an individual spin in the conformations A and B are exponentially distributed, with probability densities  $\rho_A(\tau)$  and  $\rho_B(\tau)$ , respectively:

$$\rho_A(\tau) = k_{A \rightarrow B} \exp(-\tau k_{A \rightarrow B}) \text{ and } \rho_B(\tau) = k_{B \rightarrow A} \exp(-\tau k_{B \rightarrow A}). \quad (5)$$

The expectation value for the macroscopic magnetization in the x-direction,  $M_x$ , is given by

$$M_x(t) = \sum_{j=1}^n \langle \psi_j(t) | I_{jx} | \psi_j(t) \rangle, \quad (6)$$

where  $|\psi_j(t)\rangle$  denotes the state vector of spin  $j$  at time  $t$ . We assumed that all spins are aligned in the x-direction at  $t = 0$ , and that the probability that the spin  $j$  is initially in conformation A is given by  $p_A = k_{B \rightarrow A} / (k_{A \rightarrow B} + k_{B \rightarrow A})$ . Because the Hamiltonian in expression 3 is time independent between exchange events,  $|\psi_j(t)\rangle$  can be calculated, for example, for the situation where the spin  $j$  is initially in conformation A and there are exchange events according to Eq. 4 at the times  $t_1 < t_2 < \dots < t_m$  ( $m$  odd), with  $t_1 > 0$  and  $t_m < t$ :

$$|\psi_j(t)\rangle = e^{-iH_{jB}(t-t_m)} e^{-iH_{jA}(t_m-t_{m-1})} \dots e^{-iH_{jB}(t_2-t_1)} e^{-iH_{jA}t_1} |\psi_j(0)\rangle, \quad (7)$$

where  $H_{jA} = \omega_{1j} I_{jx} + \Omega_A I_{jz}$  and  $H_{jB} = \omega_{1j} I_{jx} + \Omega_B I_{jz}$ .

For the simulation for BPTI at 36 °C, we used the correlation time for the conformational exchange,  $\tau_{ex}$ , and the product  $p_A p_B \Delta \Omega^2$ , which had been determined from fitting Eq. 1 to the experimental rotating frame relaxation times. Furthermore, use of the  $\Omega_A$  and  $\Omega_B$  values measured at temperatures below 20 °C (Otting, G., Liepinsh, E. and Wüthrich, K., unpublished results) enabled us to calculate  $p_A$  and  $p_B$  from the product  $p_A p_B \Delta \Omega^2$  and the exchange rate constants  $k_{A \rightarrow B}$  and  $k_{B \rightarrow A}$  (Eq. 2). The simulation yielded the time course of  $M_x$  (Eqs. 6 and 7), from which the exchange contribution to the relaxation in the rotating frame,  $T_{1\rho}^{sim}$ , was determined by a least-squares fit of a single exponential function. The relaxation times were finally calculated for all experimental  $\omega_1$  values, using the relation

$$\frac{1}{T_{1\rho}^{calc}} = \frac{1}{T_{1\rho}^{sim}} + \frac{1}{T_{1\rho}^{\infty}}.$$

$T_{1\rho}^{\infty}$  denotes the relaxation time in the rotating frame for infinite spin-lock power as obtained from the experimental rotating frame relaxation times after fitting to Eq. 1.

## NMR EXPERIMENTS

A 5 mM solution of uniformly  $^{15}\text{N}$ -labeled BPTI in 90%  $\text{H}_2\text{O}$ /10%  $\text{D}_2\text{O}$  was used at a temperature of 36 °C and pH = 4.6. The NMR experiments were performed on Bruker AM500 and AM360 spectrometers. The  $^{15}\text{N}$  resonance assignments of Glushka et al. (1989) were verified in a 500-MHz TOCSY-relayed- $^{15}\text{N}$ ,  $^1\text{H}$ -COSY experiment (Otting and Wüthrich, 1988).

Relaxation times were measured with the pulse schemes shown in Fig. 1, where  $^{15}\text{N}$  broadband-decoupling during proton detection was achieved by using Waltz-16 (Shaka et al., 1983). Ten different relaxation delays ( $t_{\text{rel}} = 42.5, 82.5, 112.5, 202.5, 282.5, 382.5, 482.5, 582.5, 682.5$  and  $782.5$  ms) were used to measure the longitudinal relaxation time,  $T_1$ . During the relaxation delay, the proton resonances were saturated with a train of  $90^\circ$  pulses at 5-ms intervals, as proposed by Nirmala and Wagner (1989) and Peng and Wagner (1992) to suppress the cross-correlation of dipolar and CSA relaxation (Goldman, 1984; Boyd et al., 1990; Kay et al., 1992; Palmer et al., 1992). Decoupling during  $t_1$  was achieved with Waltz-16. Transverse relaxation times,  $T_2$ , were determined with the pulse scheme of Fig. 1B, using 12 different relaxation delays ( $t_{\text{rel}} = 9, 20, 30, 40, 50, 70, 80, 100, 120, 140, 200$  and  $280$  ms). To suppress evolution of anti-phase magnetization of the  $^{15}\text{N}$ -nuclei with respect to the amide protons, we applied Waltz-16 (Shaka et al., 1983) during the relaxation delay. Waltz-16 was also used to decouple the amide protons during the chemical shift evolution of the  $^{15}\text{N}$  nuclei. Since the CW spin-lock decouples  $^{15}\text{N}$  nuclei and amide protons during the relaxation delay when measuring  $T_{1\rho}(\omega_1)$  (Fig. 1C), Waltz-16 was applied only during  $t_1$ .  $T_{1\rho}(\omega_1)$  was determined at ten different values of the CW spin-lock power ( $\omega_1 = 1210, 1960, 3140, 4130, 5060, 5820, 6830, 8490, 11220$  and  $15240$  rad  $\text{s}^{-1}$ ). At each power level, eight different relaxation delays were used ( $t_{\text{rel}} = 20, 40, 60, 80, 100, 140, 180$  and  $260$  ms). The relaxation measurements described so far were all performed at 500 MHz, but to assess the contributions from CSA,  $T_1$ ,  $T_2$  and  $T_{1\rho}$  were also measured at 360 MHz. For  $T_1$  the same relaxation delays were used at 360 MHz as at 500 MHz.  $T_2$  values at 360 MHz were obtained from measurements with  $t_{\text{rel}} = 9, 20, 30, 40, 60, 80, 100, 140, 200$  and  $280$  ms, and for  $T_{1\rho}$  measurements at 360 MHz the maximum spin-lock field achievable on our instrument was used, i.e.,  $\omega_1 = 11640$  rad  $\text{s}^{-1}$ , and  $t_{\text{rel}} = 30, 40, 50, 60, 80, 100, 140, 240$  and  $340$  ms.

The 2D spectra were recorded as  $256 \times 1024$  real matrices with 8 scans per  $t_1$  value, resulting in a total recording time of 5 days for a total of 131 experiments. The water signal was suppressed with two spin-lock purge pulses of 500  $\mu\text{s}$  and 2000  $\mu\text{s}$  duration, respectively (Fig. 1 A–C) (Messerle et al., 1989). For the  $T_{1\rho}$  measurements, the spin-lock purge pulses were applied *before* the relaxation delay,  $t_{\text{rel}}$ , (Fig. 1C), in order to avoid heteronuclear cross-polarization in the rotating frame (Maudsley et al., 1977). Quadrature detection in  $\omega_1$  was achieved by using TPPI (Marion and Wüthrich, 1983). Before Fourier transformation, the data were multiplied with a sine-bell window shifted by  $\pi/2$  (DeMarco and Wüthrich, 1976). Baseline corrections with third-order polynomials were applied in each dimension, using standard Bruker software on a Bruker X32 workstation. The peak volumes were determined by using the EASY program (Eccles et al., 1991). The relaxation times were determined by fitting a single exponential function to the peak volumes by a least-squares fit routine. Finally, the rotating frame relaxation times of the backbone  $^{15}\text{N}$  nuclei of Cys<sup>38</sup> and Arg<sup>39</sup> were fitted to Eq. 1, using the Levenberg–Marquardt algorithm (Press et al., 1986), yielding  $\tau_{\text{ex}}$ ,  $1/T_{1\rho}^\infty$ , and the product,  $p_A p_B \Delta\Omega^2$ .

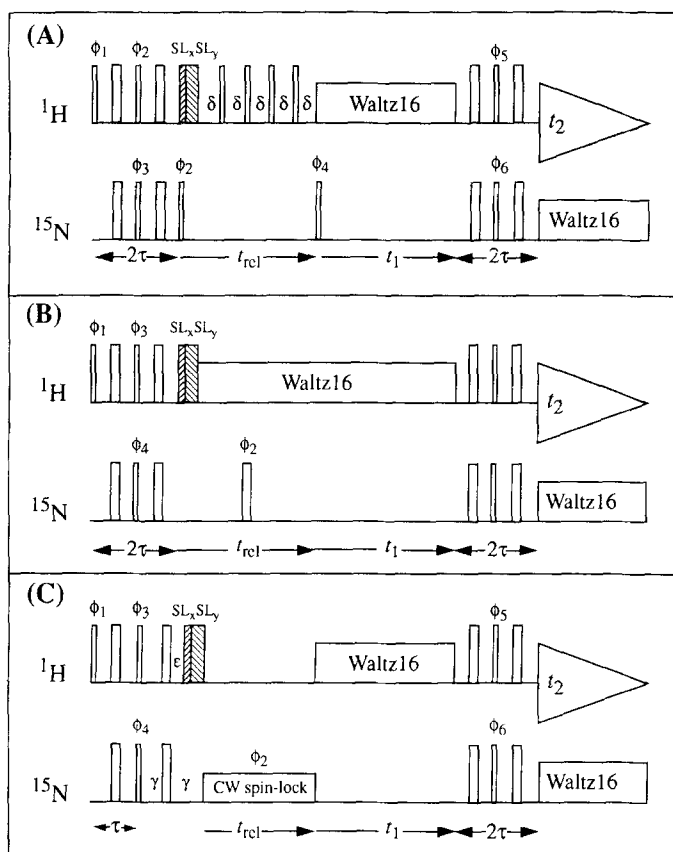


Fig. 1. Experimental schemes used for measurements of  $T_1$  (A),  $T_2$  (B) and  $T_{1\rho}$  (C) of  $^{15}\text{N}$  in polypeptide backbone amide groups.  $^1\text{H}$  pulses are shown in the upper and  $^{15}\text{N}$  pulses in the lower traces.  $90^\circ$  and  $180^\circ$  pulses are indicated by thin and thick vertical bars, respectively. Spin-lock purge pulses used to suppress the water signal are denoted as  $\text{SL}_x$  and  $\text{SL}_y$ , with pulse lengths of  $\text{SL}_x = 500 \mu\text{s}$  and  $\text{SL}_y = 2000 \mu\text{s}$ . The delay  $\tau$  was tuned to  $1/2J(^1\text{H}, ^{15}\text{N})$ . In (A) the delays  $\delta$  were set to 5 ms. In (C) the delays  $\gamma$  and  $\epsilon$  were tuned to  $\gamma + \epsilon = \tau$  and  $\gamma - \epsilon = \text{SL}_x + \text{SL}_y$ . In all three schemes, a Waltz-16 composite pulse decoupling sequence was applied during the proton detection period. The relaxation delays are indicated as  $t_{\text{rel}}$ . Phase cycling for (A):  $\phi_1 = 8(x)$ ,  $\phi_2 = 4(y, -y)$ ,  $\phi_3 = 4(x, -x)$ ,  $\phi_4 = 2(x, x, -x, -x)$ ,  $\phi_5 = 4(x)$ ,  $4(-x)$ ,  $\phi_6 = 4(y)$ ,  $4(-y)$ , receiver =  $2(x -x, -x, x, x)$ ; for (B):  $\phi_1 = 8(x)$ ,  $\phi_2 = 2(x, -x, y, -y)$ ,  $\phi_3 = 4(y)$ ,  $4(-y)$ ,  $\phi_4 = 4(x)$ ,  $4(-x)$ , receiver =  $2(x -x, x, -x)$ ; for (C):  $\phi_1 = 8(x)$ ,  $\phi_2 = 4(x, -x)$ ,  $\phi_3 = 2(y, y, -y, -y)$ ,  $\phi_4 = 2(x, x, -x, -x)$ ,  $\phi_5 = \phi_6 = 4(x)$ ,  $4(-x)$ , receiver =  $8(x)$ . The phases of all other pulses were set to  $x$ . TPPI (Marion and Wüthrich, 1983) may be achieved by simultaneous incrementation of the phases of all  $^{15}\text{N}$  pulses before the evolution time,  $t_1$ .

## RESULTS AND DISCUSSION

The analysis of the rotating frame relaxation times for the backbone  $^{15}\text{N}$  nuclei of BPTI enabled the characterization of three different types of motion, namely the overall rotational tumbling of the molecule and two internal motional modes observed at residues 14–16 and at residues 38–39, respectively.

### *Determination of the correlation time for overall rotational tumbling of BPTI in aqueous solution*

The correlation time,  $\tau_R$ , for the overall rotational tumbling of BPTI at 36 °C and pH = 4.6 was calculated from the average of the relaxation times,  $T_1^{\text{av}}$  and  $T_{1\rho}^{\text{av}}$ , of the residues 18–24 and 29–36, which form a centrally located  $\beta$ -sheet (Deisenhofer and Steigemann, 1975; Berndt et al., 1992). The off-resonance angles,  $\beta$ , (Eq. 13 in Peng and Wagner, 1992) for these residues were all between 72° and 99° for the  $T_{1\rho}$  measurements at the highest spin-lock power used ( $\omega_1 = 15240 \text{ rad s}^{-1}$ ). Therefore, off-resonance effects were neglected (Peng et al., 1991a) and a value of  $\beta = 90^\circ$  was used in all the calculations. In accordance with Kay et al. (1989), we also neglected possible contributions from fast internal motions, since residues in  $\beta$ -sheets are generally characterized by  $S \sim 1$ , where  $S$  is the order parameter (Lipari and Szabo, 1982; Kay et al., 1989; Clore et al., 1990; Stone et al., 1992). Assuming isotropic reorientation characterized by a Lorentzian spectral density function,  $J(\omega)$  (Abragam, 1961), we calculated  $\tau_R$  either for the (hypothetical) situation that the relaxation was entirely by dipolar interactions with the directly bonded amide proton (Peng et al., 1991), or with inclusion of CSA relaxation on the basis of Eq. 13 in Peng and Wagner (1992), thereby neglecting the cross-correlation of dipolar and CSA relaxation (Goldman, 1984). It has been shown that the  $^{15}\text{N}$  chemical shift tensor is axially symmetric, and we set  $\Delta\sigma = \sigma_{\parallel} - \sigma_{\perp} = -160 \text{ ppm}$  (Hiyama et al., 1988) in Eq. 13 of Peng and Wagner (1992).  $\sigma_{\parallel}$  and  $\sigma_{\perp}$  are the parallel and perpendicular components of the  $^{15}\text{N}$  chemical shift tensor. The bond length between the amide proton and the  $^{15}\text{N}$  nucleus was set to  $r_{\text{NH}} = 1.02 \text{ \AA}$  (Keiter, 1986) in Eq. 13 of Peng and Wagner (1992).

In principle, two different  $\tau_R$  values may correspond to the same value for the  $T_1$  relaxation time (Eq. 88 on p.295 in Abragam, 1961). Comparison of the measurements at 360 MHz and 500 MHz enabled us to discriminate between the two possible solutions, because as the CSA interactions are dependent on  $B^2$  (Eq. 141 on p.316 in Abragam, 1961), the CSA relaxation becomes more important at higher field strengths. At 500 MHz the CSA interactions are expected to account for approximately 30% of the  $T_1$  and  $T_{1\rho}$  relaxation (Table 1). Further inspection of Table 1 shows that the  $\tau_R$  values derived from  $T_1$  and  $T_{1\rho}$  coincide within the experimental error, yielding  $\tau_R = 2.0 \pm 0.5 \text{ ns}$ . Since we suppressed cross-correlation of dipolar and CSA relaxation for the  $T_1$  measurements but not for the  $T_{1\rho}$  measurements, we conclude that, in the framework of the present investigation, these cross-correlation effects are indeed negligible. In order to check for possible effects on the determination of the overall rotational correlation time which might arise from fast segmental motions characterized by the order parameters  $S$ , we also calculated  $\tau_R$  from the ratio  $T_1/T_{1\rho}$  (Kay et al., 1989). No significant differences were found relative to the  $\tau_R$  values calculated from  $T_1$  or  $T_{1\rho}$  alone (Table 1).

Richarz et al. (1980) obtained a value of  $\tau_R = 4 \text{ ns}$  for BPTI at 36 °C from  $^{13}\text{C}$  relaxation times. However, these earlier measurements were obtained at a protein concentration of 25 mM, where the viscosity is significantly higher than in the solutions used in the present studies.  $\tau_R = 2.0 \text{ ns}$  is also close to the value that has been estimated from the Stokes–Einstein relation for a spherical protein with a molecular weight similar to that of BPTI and with a hydration shell 2.5 Å thick in a solution with the viscosity of  $\text{H}_2\text{O}$  (Abragam, 1961; Richarz et al., 1980).

### *Investigation of intramolecular conformational exchange in BPTI*

The longitudinal relaxation times,  $T_1$ , of the individual backbone  $^{15}\text{N}$  nuclei of BPTI were longer than 380 ms throughout the amino acid sequence and, with the single exception of the

C-terminus, varied only within a narrow range for all residues (Fig. 2A). In contrast, the transverse relaxation times,  $T_2$ , for the residues 14–16, 36, and 38–40 were significantly shorter than those for the residues in the regular secondary structures (Fig. 2B), indicating that an additional rate process affects the spin relaxation of these residues. With the highest spin-lock power achievable on our instrument ( $\omega_1 = 15240 \text{ rad s}^{-1}$ ), the  $T_{1\rho}$  values of residues 36 and 38–40 were equal to those for the residues in the  $\beta$ -sheet (Fig. 2C). From Eq. 1 it follows that the correlation time of the exchange process manifested in the transverse  $^{15}\text{N}$  relaxation of these residues must be longer than 0.1 ms. A different behavior was observed for residues 14–16, which had shorter  $T_{1\rho}$  times, indicating that there must be two motional processes with different correlation times. The lower limit for the correlation time of the faster one of these processes,  $\tau_{\text{ex}}^f$ , was indicated by the observation that the  $T_1$  relaxation times of residues 14–16 were not affected (Fig. 2A), which shows that  $\tau_{\text{ex}}^f$  must be long compared to the inverse of the  $^{15}\text{N}$  Larmor frequency at 500 MHz, i.e.,  $\tau_{\text{ex}}^f \gg 3 \text{ ns}$ . (Note that Gly<sup>57</sup> and Ala<sup>58</sup> undergo intramolecular motions that were fast compared to the  $^{15}\text{N}$  Larmor frequency, so that  $T_1$ ,  $T_2$  and  $T_{1\rho}$  were all significantly increased.) An upper limit for  $\tau_{\text{ex}}^f$  may be derived from the observation that the reduction in the  $T_{1\rho}$  values of residues

TABLE 1  
CORRELATION TIMES FOR THE OVERALL ROTATIONAL TUMBLING OF BPTI IN AQUEOUS SOLUTION DETERMINED FROM MEASUREMENTS OF THE  $^{15}\text{N}$  RELAXATION TIMES  $T_1$ ,  $T_2$ ,  $T_{1\rho}$  AT  $36^\circ\text{C}^a$

Measurement	$T_{\text{av}}^b$ [ms]	$\tau_R$ [ns]	
		dipolar <sup>c</sup>	dipolar + CSA <sup>d</sup>
$T_1$ [11.7 T] <sup>e</sup>	$414 \pm 22$	$2.5 \pm 0.7$ ( $4.0 \pm 1.1$ )	$1.5 \pm 0.3$ ( $6.3 \pm 0.9$ )
$T_1$ [8.4 T] <sup>e</sup>	$336 \pm 25$	$2.5 \pm 0.6$ ( $7.5 \pm 1.5$ )	$2.0 \pm 0.5$ ( $9.0 \pm 2.2$ )
$T_{1\rho}$ [11.7 T] <sup>f</sup>	$274 \pm 9$	$2.3 \pm 0.3$	$1.8 \pm 0.3$
$T_{1\rho}$ [8.4 T] <sup>g</sup>	$252 \pm 9$	$2.3 \pm 0.3$	$2.0 \pm 0.3$
$T_1/T_{1\rho}$ [11.7 T]		$2.2 \pm 0.4$	$2.2 \pm 0.4$
$T_1/T_{1\rho}$ [8.4 T]		$1.8 \pm 0.9$	$1.9 \pm 0.8$
$T_2$ [11.7 T]	$194 \pm 12$	$3.7 \pm 0.7$	$2.8 \pm 0.6$
$T_2$ [8.4 T]	$204 \pm 10$	$3.0 \pm 1.1$	$2.6 \pm 0.6$

<sup>a</sup> The protein concentration was 5 mM, pH = 4.6. Isotropic rotational tumbling was assumed in the calculation of  $\tau_R$ . The error in the determination of  $\tau_R$  was estimated from the longest and shortest measured relaxation times.

<sup>b</sup> Average of the relaxation times measured for the residues 18–24 and 29–35, which are all located in a  $\beta$ -sheet in the solution structure of BPTI (Wagner et al., 1987; Berndt et al., 1992). The errors represent the standard deviation of the relaxation times determined for these residues.

<sup>c</sup> Correlation time,  $\tau_R$ , calculated on the assumption that the measured relaxation rate was due entirely to dipolar relaxation.

<sup>d</sup> Dipolar coupling and chemical shift anisotropy interactions were considered. The two relaxation pathways were assumed to be uncorrelated.

<sup>e</sup> The determination of  $\tau_R$  from  $T_1$  relaxation times yielded two solutions at any given field strength. The values that were excluded from comparison of the results obtained at different field strengths are given in parentheses.

<sup>f</sup> Relaxation times obtained with the highest spin-lock power used ( $\omega_1 = 15240 \text{ rad s}^{-1}$ ; see text).

<sup>g</sup>  $\omega_1 = 11640 \text{ rad s}^{-1}$ .



14–16 relative to those observed for residues in the  $\beta$ -sheet was virtually identical to that of the corresponding  $T_2$  values. Thus, the  $T_{1\rho}$  values of residues 14–16 appeared to be independent of  $\omega_1$  for  $0 \leq \omega_1 \leq 15240 \text{ rad s}^{-1}$ , so that  $0.1 \text{ ms} \gg \tau_{\text{ex}}^f \gg 3 \text{ ns}$ .

For a quantitative determination of the correlation time for the conformational exchange at residues 36 and 38–40,  $\tau_{\text{ex}}^s$ , we measured the rotating frame relaxation times as a function of the spin-lock power. We set the carrier in the  $^{15}\text{N}$  dimension at 115.5 ppm, which is equidistant from the  $^{15}\text{N}$  chemical shifts of Cys<sup>38</sup> (114.8 ppm) and Arg<sup>39</sup> (116.2 ppm). Thus, off-resonance effects for observations with these two residues were minimized. (Figure 2B shows that the  $T_2$  relaxation times of Cys<sup>38</sup> and Arg<sup>39</sup> were about 10 times shorter than those of rigidly embedded residues, which is the most pronounced manifestation of chemical exchange processes in the entire protein. The following experiments therefore focused on these two residues). At the lowest spin-lock power used ( $\omega_1 = 1210 \text{ rad s}^{-1}$ ), the angle,  $\beta$ , was  $80^\circ$  for both residues. The dependence of the decay rate constants of the magnetization in the rotating frame,  $1/T_{1\rho}$ , on the Larmor frequency of the spin-lock field for Cys<sup>38</sup> (Fig. 3A) and Arg<sup>39</sup> (Fig. 3B) was fitted to Eq. 1. The resulting parameters are shown in Table 2. The correlation times obtained for the slower of the two conformational exchange processes,  $\tau_{\text{ex}}^s$ , coincided within the accuracy of the measurements, i.e., they were  $2.4 \pm 1.8 \text{ ms}$  for Cys<sup>38</sup> and  $1.3 \pm 0.5 \text{ ms}$  for Arg<sup>39</sup>. The observation that the rotating frame relaxation times at infinite spin-lock power,  $T_{1\rho}^\infty$ , were in the same range as those for rigidly embedded residues (Fig. 2C) supports the notion that the short  $T_2$  relaxation times for residues 38 and 39 (Fig. 2B) were solely due to a local conformational exchange process.

It has been shown (Otting, G., Liepinsh, E. and Wüthrich, K., unpublished results) that BPTI in solution exchanges between two conformations, A and B, which differ in the chirality of the Cys<sup>14</sup>–Cys<sup>38</sup> disulfide bond. The activation parameters of the conformational exchange in the temperature range  $4^\circ\text{C}$  to  $16^\circ\text{C}$  were determined by longitudinal two-spin order exchange difference spectroscopy (Wider et al., 1991). In order to investigate whether the exchange-broadening of the  $^{15}\text{N}$  resonances of Cys<sup>38</sup> and Arg<sup>39</sup> at  $36^\circ\text{C}$  can be attributed to this disulfide bond isomerization, we compared the present results with those found by Otting, Liepinsh and Wüthrich (unpublished results) for the population of the major component,  $p_A$ , and the rate constant,  $k_{A \rightarrow B}$ , for the disulfide flip at  $36^\circ\text{C}$ . Table 2 shows that this estimate of the parameters was close to the data measured, which suggests that disulfide bond isomerization is indeed the conformational exchange process that causes the short  $T_2$  relaxation times observed for residues 38 and 39. The deviations between the estimated values and the measured data for the product  $p_A p_B \Delta\Omega^2$  for Arg<sup>39</sup> are possibly due to changes in the chemical shift difference,  $\Delta\Omega$ , when the temperature is increased from  $16^\circ\text{C}$  to  $36^\circ\text{C}$ . For residues 14–16, where one would also expect to observe the influence of disulfide bond isomerization, these effects were apparently masked by an additional, faster rate process.

#### *Simulation of the exchange contribution to the rotating frame relaxation*

Using the experimental correlation time,  $\tau_{\text{ex}}^s$ , and chemical shift differences,  $\Delta\Omega$ , we found that  $\Delta\Omega\tau_{\text{ex}}^s(\text{Cys}^{38}) = 0.7$  and  $\Delta\Omega\tau_{\text{ex}}^s(\text{Arg}^{39}) = 1.5$ . Since Eq. 1 was derived from second-order perturbation theory on the assumption that  $\Delta\Omega\tau_{\text{ex}} \ll 1$ , its validity for the system studied needed to be re-examined (see also p.282 of Abragam, 1961). Another approximation in the derivation of Eq. 1, which is not strictly valid in the present example, is that off-resonance effects were not considered. The observed average  $^{15}\text{N}$  chemical shift,  $\bar{\Omega}$ , is related to the chemical shifts of the major and

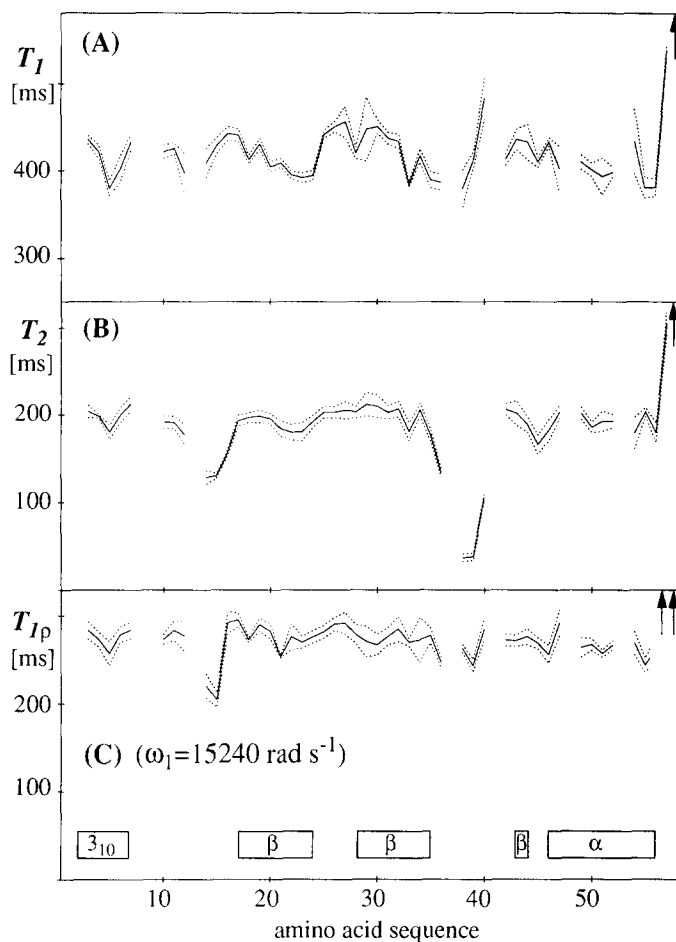


Fig. 2. Plots of the relaxation times  $T_1$  (A),  $T_2$  (B) and  $T_{1\rho}$  (C) of  $^{15}\text{N}$  in backbone amide groups of BPTI versus the amino acid sequence (solid line). Values that went off-scale are indicated by arrows. The dotted lines represent the 99% confidence interval corresponding to  $2.5\sigma$ , where  $\sigma$  is the standard deviation of the determination of the relaxation times. The measurements were made at 36 °C in a 5 mM aqueous solution of BPTI, pH = 4.6. At the bottom, the sequence locations of regular secondary structures in the solution conformation of BPTI are indicated, where  $3_{10}$  and  $\alpha$  identify the corresponding helix types, and  $\beta$  the individual strands of an antiparallel  $\beta$ -sheet.

minor conformers, A and B by  $\bar{\Omega} = p_A\Omega_A + p_B\Omega_B$ . Given that  $\bar{\Omega}(\text{Cys}^{38}) = -220 \text{ rad s}^{-1}$  and  $\bar{\Omega}(\text{Arg}^{39}) = 220 \text{ rad s}^{-1}$ , one obtains with  $\Delta\Omega(\text{Cys}^{38}) = 542 \text{ rad s}^{-1}$  and  $\Delta\Omega(\text{Arg}^{39}) = 1150 \text{ rad s}^{-1}$  that  $\Omega_A(\text{Cys}^{38}) = -133 \text{ rad s}^{-1}$ ,  $\Omega_B(\text{Cys}^{38}) = -675 \text{ rad s}^{-1}$ ,  $\Omega_A(\text{Arg}^{39}) = 300 \text{ rad s}^{-1}$ , and  $\Omega_B(\text{Arg}^{39}) = -850 \text{ rad s}^{-1}$ . The corresponding tip angles of the spin-lock axis for the major and minor conformers,  $\beta_A$  and  $\beta_B$ , were 76° and 55° for  $\text{Arg}^{39}$ , and 84° and 61° for  $\text{Cys}^{38}$ , respectively. Thus, although the off-resonance effect would be negligibly small for the *average* resonance frequency, under the experimental conditions chosen, the minor conformer experienced a significantly larger off-resonance effect for both residues.

To check the validity of Eq. 1 for the present system, we simulated the relaxation in the rotating

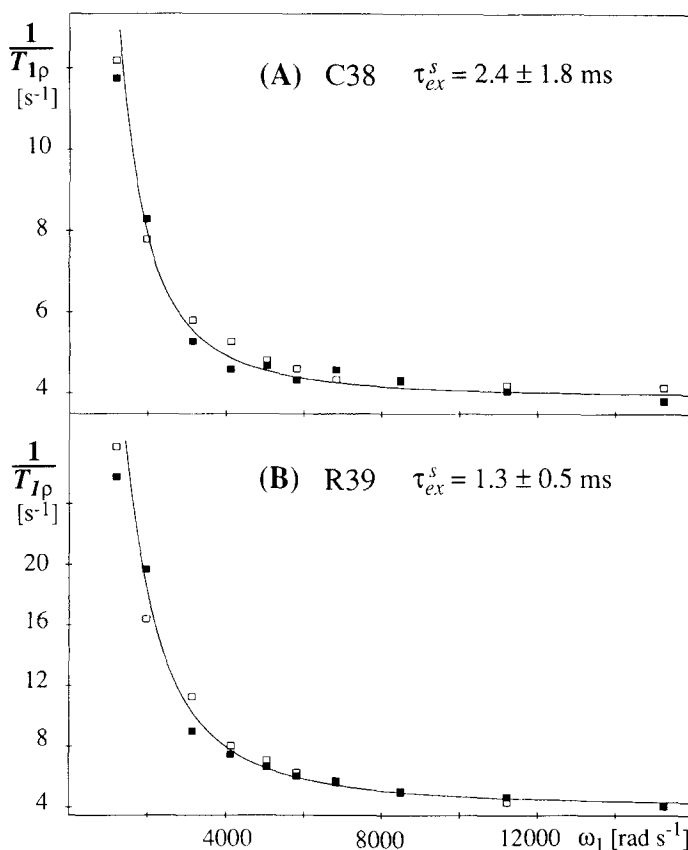


Fig. 3. Plots of the inverse of the measured  $^{15}\text{N}$  rotating frame relaxation times,  $T_{1\rho}$ , (filled squares) versus the spin-lock power,  $\omega_1$ , and comparison with the  $T_{1\rho}$  model calculations described in the text (open squares). The solid curves represent fits of Eq. 1 to the experimental data; the correlation times for conformational exchange,  $\tau_{\text{ex}}^s$ , obtained from this fitting procedure are also indicated.

frame arising from conformational exchange on the basis of a rigorous quantum-mechanical treatment (see Theory). We applied the parameters obtained using second-order perturbation theory (Table 2) and the chemical shift differences measured at 16 °C (Otting, G., Liepinsh, E. and Wüthrich, K., unpublished results). The calculated rotating frame relaxation times are shown in Fig. 3. Comparison with the experimental data (Fig. 3) demonstrates that the parameters obtained from Eq. 1 were correct, which implies that time-dependent perturbation theory is quite robust with respect to violations of the inequality  $\Delta\Omega\tau_{\text{ex}} \ll 1$ . Furthermore, calculation of the line shape for a two-site exchange, using the kinetic parameters and the chemical shift difference of  $\text{Arg}^{39}$  in Table 2 with the equations of Gutowsky and Saika (1953), showed that a single, coalesced resonance line was indeed expected for  $\text{Arg}^{39}$ . In contrast, two signals were expected when the product  $\Delta\Omega\tau_{\text{ex}}^s$  was doubled, by increasing either  $\tau_{\text{ex}}$  or  $\Delta\Omega$  by a factor of 2, and the transverse magnetization displayed oscillatory behavior in simulations with  $\Delta\Omega\tau_{\text{ex}}^s \gg 1$ . The present results thus suggest that the commonly used second-order perturbation theory is a good

approximation whenever coalesced resonance lines are observed. On the basis of the close coincidence of the experimental and simulated data sets (Fig. 3), it appears that the influence of even rather large off-resonance effects (see above) is negligibly small.

*Comparison of the absolute values for the relaxation times  $T_{1\rho}$  and  $T_2$*

$T_{1\rho}$  relaxation times were in general longer than the corresponding  $T_2$  relaxation times (Fig. 2B and C), although, in the absence of chemical exchange processes (Peng and Wagner, 1992) and evolution of antiphase magnetization (Peng et al., 1991b), they were expected to be equal. As discussed by Peng and Wagner (1992), cross-correlation between dipolar relaxation and CSA relaxation may lead to longer  $T_{1\rho}$  values. However, the close agreement between the correlation times for overall rotational tumbling,  $\tau_R$ , obtained from  $T_1$  and  $T_{1\rho}$  measurements, respectively (Table 1), indicates that such cross-correlation effects were negligible within the framework of the present investigation. Thus, the apparent discrepancy in the present measurements can probably be attributed to the use of the composite pulse decoupling scheme, Waltz-16 (Shaka et al., 1983), during the relaxation delay in the  $T_2$  measurements (Fig. 1B). It has recently been reported by Kay et al. (1992) that the  $^{15}\text{N}$  transverse magnetization decay rate is increased if composite pulse sequences are applied during the relaxation delay, since the scalar coupling between amide protons and  $\alpha$ -protons diminishes the quality of the heteronuclear decoupling sequence and thus leads to incomplete heteronuclear decoupling (see also Shaka et al., 1988). The artifactually shortened  $T_2$  relaxation times would correspond to longer apparent correlation times for the overall rotational tumbling,  $\tau_R$ . Table 1 shows that the  $\tau_R$  values derived from the  $T_2$  relaxation

TABLE 2  
PARAMETERS CHARACTERIZING THE CONFORMATIONAL EXCHANGE OBSERVED FOR RESIDUES CYS<sup>38</sup> AND ARG<sup>39</sup> IN BPT1<sup>a</sup>

Residue	$\tau_{\text{ex}}^a$ [ms] <sup>b</sup>	$T_{1\rho}^{\infty}$ [ms] <sup>c</sup>	$p_A p_B \Delta\Omega^2$ [rad <sup>2</sup> s <sup>-2</sup> ] <sup>d</sup>	$p_A^{d,e}$	$k_{A \rightarrow B}^{d,f}$ [s <sup>-1</sup> ]
<b>Cys<sup>38</sup></b> <sup>f</sup>	<b>2.4 ± 1.8</b>	<b>256 ± 3</b>	<b>39000 ± 27000</b>	<b>0.84</b>	<b>66</b>
Estimate <sup>g</sup>	1.3 ± 0.7		11000 ± 3000	0.96 ± 0.01	40 ± 20
<b>Arg<sup>39</sup></b> <sup>f</sup>	<b>1.3 ± 0.5</b>	<b>245 ± 3</b>	<b>83000 ± 5000</b>	<b>0.93</b>	<b>53</b>
Estimate <sup>g</sup>	1.3 ± 0.7		51000 ± 13000	0.96 ± 0.01	40 ± 20

<sup>a</sup> Protein concentration 5 mM, T = 36 °C, pH = 4.6.

<sup>b</sup> Correlation time for the slow conformational exchange process (see text).

<sup>c</sup> Rotating frame relaxation time in the limit of infinite spin-lock power.

<sup>d</sup> Site A denotes the major conformer.

<sup>e</sup> The chemical shift difference  $\Delta\Omega$  was set to the value observed at 16 °C, i.e., for Cys<sup>38</sup>,  $\Delta\Omega = 540 \text{ rad s}^{-1}$ , and for Arg<sup>39</sup>,  $\Delta\Omega = 1150 \text{ rad s}^{-1}$  (Otting, G., Liepinsh, E. and Wüthrich, K., unpublished results).

<sup>f</sup> The experimental results are listed with bold numbers. They were determined from  $^{15}\text{N}$  rotating frame relaxation time measurements, using a non-linear fit to Eq. 1.

<sup>g</sup>  $\tau_{\text{ex}}^a$  was computed with Eq. 1 from the values of  $p_A$  and  $k_{A \rightarrow B}$  derived from the amide proton line widths measured at 36 °C for the residues 14–18 and 38–41, which were all affected by the isomerization of the disulfide bond Cys<sup>14</sup>–Cys<sup>38</sup> (Fig. 2B), and using values of  $\Delta\Omega$  measured at 16 °C (Otting, G., Liepinsh, E. and Wüthrich, K., unpublished results). The interpretation of these proton line widths was based on the assumption that there was an exchange process between two isomeric states. The use of  $p_A = 0.96$  at 36 °C was based on extrapolation from measurements in the temperature range 4 °C to 16 °C and at 68 °C (Otting, G., Liepinsh, E. and Wüthrich, K., unpublished results).

times obtained with the experimental scheme of Fig. 1B were indeed significantly longer than those derived from  $T_1$  or  $T_{1\rho}$ .

## CONCLUSIONS

The present investigation demonstrated that measurement of rotating frame relaxation times as a function of the spin-lock power allows the determination of correlation times for rate processes such as conformational exchange in the millisecond range. The determination of correlation times with this method is independent of knowledge of the chemical shift differences and the relative populations of the interchanging species. Furthermore, comparison with simulated data showed that second-order perturbation theory is adequate to evaluate  $T_{1\rho}$  data within the limit  $\Delta\Omega\tau_{\text{ex}} \sim 1$ , and that off-resonance effects become important only with relatively slow exchange rates that must be measured with small spin-lock frequencies,  $\omega_1$ . On this basis, it appears that  $T_{1\rho}$  measurements of  $^{15}\text{N}$  might become an attractive tool for quantitative motional characterization of uniformly  $^{15}\text{N}$ -enriched proteins.

## ACKNOWLEDGEMENTS

Financial support was obtained from the Schweizerischer Nationalfonds (project 31.32033.91) and the Stipendien-Fonds im Verband der Chemischen Industrie (fellowship to Th.S.). We thank Bayer AG, Leverkusen, Germany, for a generous gift of  $^{15}\text{N}$ -enriched BPTI, and Mr. R. Marani for the careful processing of the manuscript.

## REFERENCES

- Allerhand, A., Doddrell, D. and Komoroski, R. (1971) *J. Chem. Phys.*, **55**, 189–198.  
 Abragam, A. (1961) *The Principles of Nuclear Magnetic Relaxation*. Clarendon Press, Oxford.  
 Berndt, K.D., Güntert, P., Orbons, L.P.M. and Wüthrich, K. (1992) *J. Mol. Biol.*, **227**, 757–775.  
 Blicharski, J.S. (1972) *Acta Phys. Pol. A*, **41**, 223–236.  
 Boyd, J., Hommel, U. and Campbell, I.D. (1990) *Chem. Phys. Lett.*, **175**, 477–482.  
 Brüscheiler, R.P. (1992) Ph.D. thesis No. 9466, ETH Zürich.  
 Clore, G.M., Driscoll, P.C., Wingfield, P.T. and Gronenborn, A.M. (1990) *Biochemistry*, **29**, 7387–7401.  
 DeMarco, A. and Wüthrich, K. (1976) *J. Magn. Reson.*, **24**, 201–204.  
 Deisenhofer, J. and Steigemann, W. (1975) *Acta Cryst.*, **B31**, 238–250.  
 Deverell, C., Morgan, R.E. and Strange, J.H. (1970) *Mol. Phys.*, **18**, 553–559.  
 Eccles, C., Güntert, P., Billeter, M. and Wüthrich, K. (1991) *J. Biomol. NMR*, **1**, 111–130.  
 Goldman, M. (1984) *J. Magn. Reson.*, **60**, 437–452.  
 Glushka, J., Lee, M., Coffin, S. and Cowburn, D. (1989) *J. Am. Chem. Soc.*, **111**, 7716–7722.  
 Gutowsky, H.S. and Saika, A. (1953) *J. Chem. Phys.*, **21**, 1688–1694.  
 Hiyama, Y., Niu, C., Silvertown, J.V., Bavoso, A. and Torchia, D.A. (1988) *J. Am. Chem. Soc.*, **110**, 2378–2383.  
 Jones, G.P. (1966) *Phys. Rev.*, **148**, 332–335.  
 Kaplan, J.I. and Fraenkel, G. (1980) *NMR of chemically exchanging systems*. Academic Press, New York.  
 Kay, L.E., Jue, T., Bangerter, B. and Demou, P.C. (1987) *J. Magn. Reson.*, **73**, 558–564.  
 Kay, L.E., Torchia, D.A. and Bax, A. (1989) *Biochemistry*, **28**, 8972–8979.  
 Kay, L.E., Nicholson, L.K., Delaglio, F., Bax, A. and Torchia, D.A. (1992) *J. Magn. Reson.*, **97**, 359–375.  
 Keiter, E.A. (1986) Ph.D. Thesis, University of Illinois.  
 Kördel, J., Skelton, N.J., Akke, M., Palmer III, A.G. and Chazin, W.J. (1992) *Biochemistry*, **31**, 4856–4866.

- Lipari, G. and Szabo, A. (1982) *J. Am. Chem. Soc.*, **104**, 4546–4559 and 4560–4570.
- Marion, D. and Wüthrich, K. (1983) *Biochem Biophys. Res. Comm.*, **113**, 967–974.
- Maudsley, A.A., Müller, L. and Ernst, R.R. (1977) *J. Magn. Reson.*, **28**, 463–469.
- Messerle, B.A., Wider, G., Otting, G., Weber, C. and Wüthrich, K. (1989) *J. Magn. Reson.*, **85**, 608–613.
- Nirmala, N.R. and Wagner, G. (1988) *J. Am. Chem. Soc.*, **110**, 7557–7558.
- Nirmala, N.R. and Wagner, G. (1989) *J. Magn. Reson.*, **82**, 659–660.
- Oppenheim, I., Shuler, K.E. and Weiss, G.H. (1977) *Stochastic Processes in Chemical Physics: The Master Equation*, MIT Press, Cambridge.
- Otting, G. and Wüthrich, K. (1988) *J. Magn. Reson.*, **76**, 569–574.
- Palmer III, A.G., Skelton, N.J., Chazin, W.J., Wright, P.E. and Rance, M. (1992) *Mol. Phys.*, **75**, 699–711.
- Peng, J.W., Thanabal, V. and Wagner, G. (1991a) *J. Magn. Reson.*, **94**, 82–100.
- Peng, J.W., Thanabal, V. and Wagner, G. (1991b) *J. Magn. Reson.*, **95**, 421–427.
- Peng, J.W. and Wagner, G. (1992) *J. Magn. Reson.*, **98**, 308–332.
- Press, W.H., Flannery, B.P., Teukolsky, S.A. and Vetterling, W.T. (1986) *Numerical Recipes*, Cambridge University Press, Cambridge.
- Richarz, R., Nagayama, K. and Wüthrich, K. (1980) *Biochemistry*, **19**, 5189–5196.
- Sandström, J. (1982) *Dynamic NMR spectroscopy*. Academic Press, New York.
- Schneider, D.M., Dellwo, M.J. and Wand, A.J. (1992) *Biochemistry*, **31**, 3645–3652.
- Sklenar, V., Torchia, D. and Bax, A. (1987) *J. Magn. Reson.*, **73**, 375–379.
- Shaka, A.J., Keeler, J., Frenkiel, T. and Freeman, R. (1983) *J. Magn. Reson.*, **52**, 335–338.
- Shaka, A.J., Lee, C.J. and Pines, A. (1988) *J. Magn. Reson.*, **77**, 274–293.
- Stilbs, P. and Moseley, M.M. (1978) *J. Magn. Reson.*, **31**, 55–61.
- Stone, M.J., Fairbrother, W.J., Palmer III, A.G., Reizer, J., Saier, M.H. and Wright, P.E. (1992) *Biochemistry*, **31**, 4394–4406.
- Wagner, G. and Wüthrich, K. (1982) *J. Mol. Biol.*, **155**, 347–366.
- Wagner, G. and Nirmala, N.R. (1989) *Chemica Scripta*, **29A**, 27–30.
- Wagner, G., Braun, W., Havel, T.F., Schaumann, T., Gö, N. and Wüthrich, K. (1987) *J. Mol. Biol.*, **196**, 611–639.
- Wider, G., Neri, D. and Wüthrich, K. (1991) *J. Biomol. NMR*, **1**, 93–98.